Al-Nahrain Journal of Science
ANJS, Vol.23 (3), September, 2020, pp. 1 – 6

Preparation and Characterization of Co Doped Copper Oxide (II) Thin Films by 45° Angle Chemical Spraying Pyrolysis

Afnan N. Hussain*, Mustafa A. Hassan and Khaleel I. Hassoon

Department of Applied Sciences, University of Technology, Baghdad, Iraq

Articles Information

Received:
18.03.2020
Accepted:
03.06.2020
Published:
26.09.2020

Keywords:
Solar Cell Application
CuO thin films
Cobalt doing
Spray Pyrolysis

Abstract

In this work, Co doped copper oxide (II) thin films (COTF) were deposited by chemical spray pyrolysis method. Structural analyses have confirmed monoclinic polycrystalline for COTF deposited at 400 ºC substrate temperature. Compared with pure COTF, Co-doped samples showed larger grain size with distortion in the structure. With the increase of doping concentration the structure changes to amorphous. Bandgap energy was 2.45 eV before doping and 2.6 eV at 3% doping and began to decrease with increasing doping concentration. Activation energy was found to be 0.24 eV and it decrease with increase of doping. The Co (6%) doped –COTF are deposited on silicon substrate to fabricate CuO-Si hetero-junction.

DOI: 10.22401/ANJS.23.3.01

*Corresponding author: afnannooraldeen@yahoo.com

1. Introduction

CuO is a one among important monoclinic III-V compounds and interesting transitional metal oxide semiconductor showing p-type conductivity [1]. CuO is used because of its non-toxic nature, and its constituents are available in Earth [2]. COTF were deposited by several methods, such as anodization method [3], Spray Pyrolysis [4], Spin coating technique [5], Sol-Gel technique [6], and Chemical bath deposition method [7].

Researchers have studied the improvement of the properties of CuO with several mechanisms, including the treatment of heat (annealing) [8], and doping with other elements to improve their characteristics. Dopants such as Lithium (Li) [9, 10, 11], Manganese (Mn) [12, 13], Zirconium (Zr) [14], and Iron (Fe) [7] used to improve the device properties for several applications.

Cobalt is already used as a dopant in COTF by many researchers recently [15, 16, 17] due to: (a) similarity in ionic radii between Co (0.082 nm) and Cu (0.096 nm) [18], (b) it's reported to be one among the primary nonprecious metal catalyst with properties quite almost similar to that of platinum [15].

Copper oxide thin films doped with cobalt are prepared in several methods: flame spray pyrolysis [19], precipitation method [20], spin coating technique [5], and sputtering technique [16] and successive ionic layer adsorption and reaction method [21].

In this work, we prepared Co- doped CuO thin film by spray pyrolysis, using different concentration 3%, 6%, and 9% of doping Co. Precise examination of structural and optical properties of Co doped CuO films, and electrical properties has been also implemented. The aim of this work is to increase the conductivity of CuO thin films by doping, which can be used as a device in solar cells applications. Our 45º angle deposition using low cost spray pyrolysis technique can provide smooth thin films with fewer defects which can enhance the performance of CuO thin film solar cells.

2. Experimental

COTF doped with Co (3%, 6%, and 9%) were deposited by spray pyrolysis method on glass substrate. Pure Cu $(NO_3)_2.3H_2O$ and Co $(NO_3)_2.6H_2O$ from PHD company were prepared in volumetric ratios by preparing the same concentration of copper nitrate and cobalt nitrate 0.1 M and dissolved in distilled water. The solutions are sprayed diagonally at 45°, for 3 s spraying time in 30 s stopping time (the time between two deposition batches). The substrates; glass and Si wafers are rotated on a hot plate with 0.12 ml/sec deposition rate at 400 ºC temperature. The (XRD) equipment utilizes Cu-Kα radiation (λ=0.15418 nm) (8 deg/min) and theta range (10-80 deg). Atomic Force Microscope (AA2000 Atomic Force Microscope AFM) has been utilized to analyze the surface topography of the films. The morphology of the film and the film thickness by cross section (FESEM) was obtained. The energy band gap E_g, and absorption coefficients were determined by UV-Vis spectrophotometer using wavelength range (400-1100 nm). The dc-electrical properties of the films were analyzed by Hall measurement system using an applied magnetic field (0.25 T) and a current in the range (0-40 μA). These measurements are

used to determine the type of charge carriers, the conductivity and the mobility of the material. Activation Energy Ea has been studied by a homemade Seebeck system.

3. Results and Discussion

Structural properties

The XRD patterns of the pure and Co-doped of all examples are presented in Figure (1). The peaks, indexed as (002) and (111) are located at 35.6 and 38.6° 2theta which correspond to (002), and (111) planes of CuO, respectively. The intensity of the (111) peak increases at doping ratio of 3%. The intensity of the (002) indexed peak decreases with the increase of doping with cobalt indicating that structural changes occur such that degree of crystalinity decreases with the doping increased. The structures of the un-doped sample have been assigned to be monoclinic polycrystalline structure. In general, the amorphous nature of the material leads to the hump-like feature in the XRD pattern. In the present work, the crystalline film was deposited on an amorphous glass substrate. The hump-like feature, observed in the XRD pattern, is believed to be due to the x-ray being diffracted by the substrate. The intensity of the XRD pattern is limited such that the (002) peak decreases and becomes hard to be observed with the increase of doping with cobalt.

The decrease of crystallinity with the increase in doping was reported for CuO thin films doped with zinc [4]. The grain size D values are (6.5, 7.8, 13.05 and 13.04 nm) for un-doped, 3%-, 6%- and 9%-doped thin films with Co respectively. The crystal size (D) increases with the increase in Co-doping of the CuO film. This is attributed to the ionic mobility and radius of cobalt ions (58.93 Å). In addition, due to the low activation energy, these ions transfer from trap sites to nucleation sites during the crystal growth process leading to increase in crystal size [5, 18]. Increasing of doping up to 3% leads to increases the grain size dramatically and suddenly result-in a distortion of the structure. These results have good agreement with FESEM images as they will be displayed later on. The conductivity of Co doped increase significantly at 9%.

The grain size of Co doped CuO thin films was determined by estimating the full peak width at half maximum (FWHM) of (111) utilizing the Scherrer's condition [22].

$$D = \frac{0.94\,\lambda}{\beta \cos\theta} \quad (1)$$

where λ is the wavelength (0.15418 nm), θ is the Bragg diffraction angle, β is the FWHM.

Bragg's law is used to determine the lattice spacing (d) for all the COTF [22]:

$$2d\ sin\theta = n\lambda \quad (2)$$

where n=1 is the principle diffraction order. The dislocation density of defects (δ) in the CuO films was determined utilizing the following equation [23]:

$$\delta = \frac{1}{D^2} \quad (3)$$

The dislocation density in the CuO structure decrease for Co doping at 3% Co (from 2.3×10^{12} to 0.58×10^{12} cm^{-2}) corresponding to more regular crystalline structure at 6%, where the dislocation density has been decreased because the grain size of film was increase with doping which means that the number of defects in the CuO films has been decreased with the doping. These results coincide with those of reference [16].

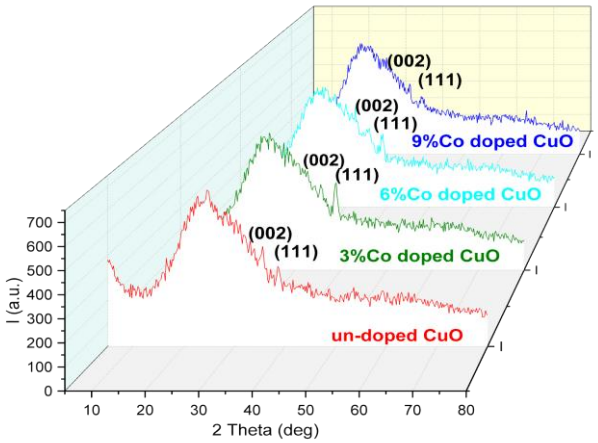

Figure 1. The X-ray diffraction (XRD) CuO Doping (3%, 6%, 9% Co).

FESEM images with scale bar 1μ and 500 nm for pure and doped 3%, 6% and 9% COTF are shown in Figures 2 (a-d). The doping of CuO thin films with Co affected the homogeneity of the films, where the homogeneity of these films decreases with an increase in the proportion of the Co, the reason may be due to an increase in the grain size as shown in Table 2. It is also noticed that with the increase of doping the nanostructures in the thin film increase due to possible transfer of Co ions to nucleation sites [4]. This is expected to result into enhancement of mobility of charge carriers due to increase of charge carriers concentration at the nucleation sites.

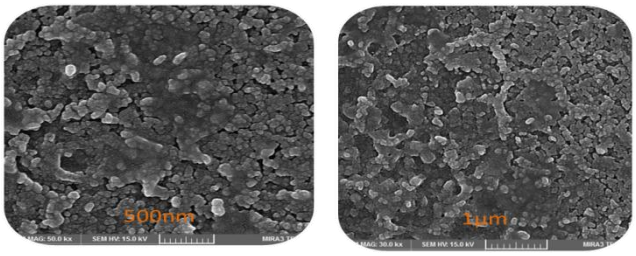

Figure 2(a). FESEM image for CuO un-doped.

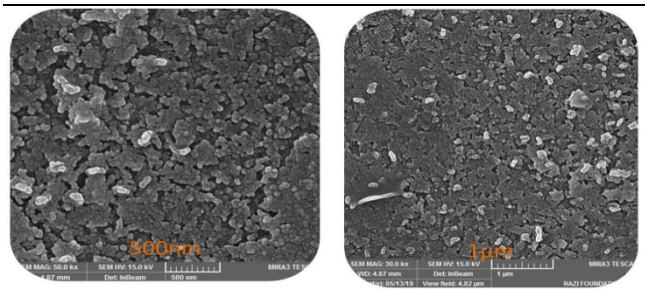

Figure 2(b). FESEM image for CuO doping 3% Co.

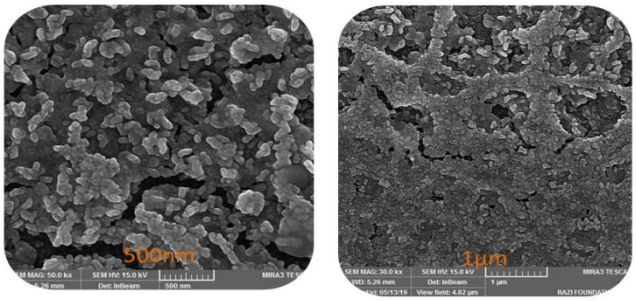

Figure 2(c). FESEM image for CuO doping 6% Co.

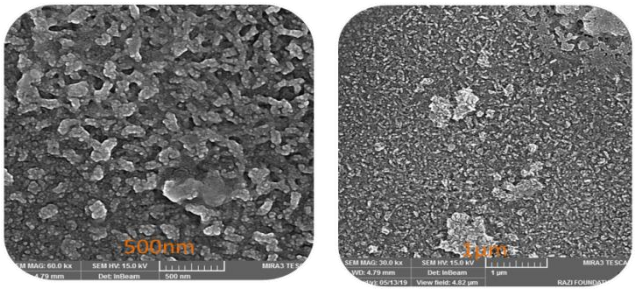

Figure 2(d). FESEM image for CuO doping 9% Co.

Topography of the films is presented by AFM 3D images in Figures 3 (a-d). In general, the particle size has a similar performance to the crystallite size. Average Roughness decrease with the increase of Co doped CuO and increases at 9%, as shown in Table 1. And these results will good aggregates with FESEM images.

Table 1. AFM parameters of CuO un-doped and Co doped.

Samples	Roughness average nm	Root mean square RMS nm
CuO- pure	4.51	5.82
3% Co	4.38	5.67
6% Co	4.18	5.36
9% Co	4.3	5.51

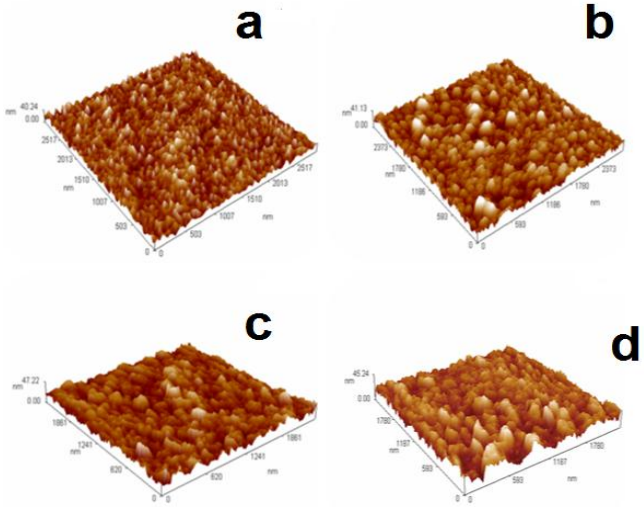

Figure 3. AFM 3-D image for (a) CuO pure,(b) CuO doping 3% Co, (c) CuO doping 6% Co, and (d) CuO doping 9% Co.

Optical properties

In Figures 4 (a-d), the values of direct energy gaps (E_g) are determined from the intercepts of the least square fits with the x-axes. The optical band gaps were (2.45, 2.6, 2.55 and 2.5eV) for un-doped, 3%, 6% and 9% Co doping CuO, respectively. In particular, E_g had a relatively high value at doping concentration of 3% Co. This may be due to enhanced crystallization of the CuO deposited films as indicated by the XRD pattern (Figure 1). However, E_g decreased at doping concentrations 6% and 9% Co and this may be due to high number of defects in the structure at this high doping concentration. This behavior agrees well with that in reference [17].

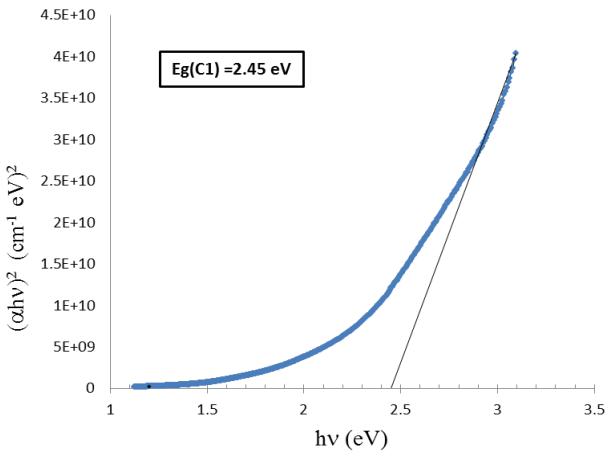

Figure 4(a). Energy bandgab for CuO thin film (C1) un-doped.

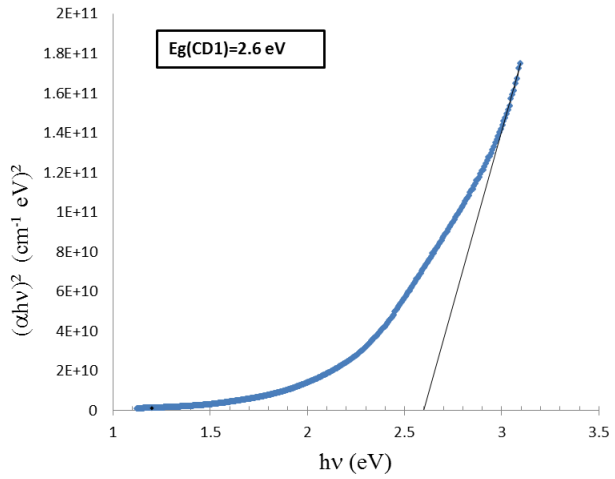

Figure 4(b). Energy bandgab for CuO thin film doping with (CD1) 3%.

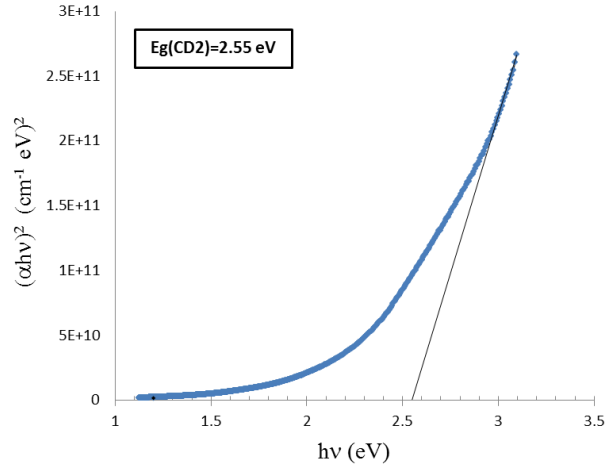

Figure 4(c). Energy bandgab for CuO thin film doping with (CD2) 6%.

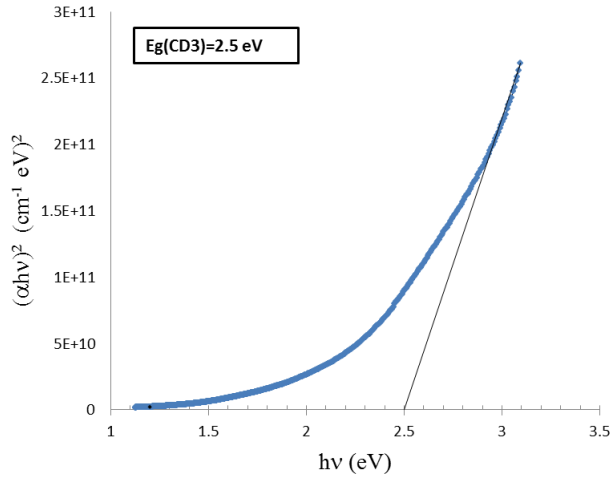

Figure 4(d). Energy bandgab for CuO thin film doping with (CD3) 9% Co.

The energy values of Urbach, which is the energy of extra levels (tails levels), are associated with the XRD characteristics are recorded in Table 2. The estimations of E_u are discovered increment, while the increase in grain size and decrease in dislocation density means an increase in the energy of the additional level E_u.

Table 2. XRD parameters calculated grain size and Dislocation density assorted with Eurbach energy.

Sample	E_u (eV)	Grain size (D)nm	Dislocation density (δ)$cm^{-2}\times10^{12}$	Activation energy E_a (eV)
CuO-pure	1.04	6.5	2.3	0.24
CuO doping 3% Co	1.08	7.8	1.6	0.12
CuO doping 6% Co	1.13	13.05	0.58	0.08
CuO doping 9% Co	1.25	13.04	0.58	0.07

Relatively low bandgab (high blackness) for Co-doped CuO is relevant to optoelectronic devices, for example, solar cell and photodiode.

Electrical properties

Activation energy E_a for Co-doped COTF are presented in Table 2. Due to doping, E_a decreases 0.24 to 0.07 eV. Fig. 5 shows a plot between 1000/T and Seeback coefficient. Decreasing of E_a with doping is confirmed by Urbach energy E_u values. Similar behavior is reported in [21].

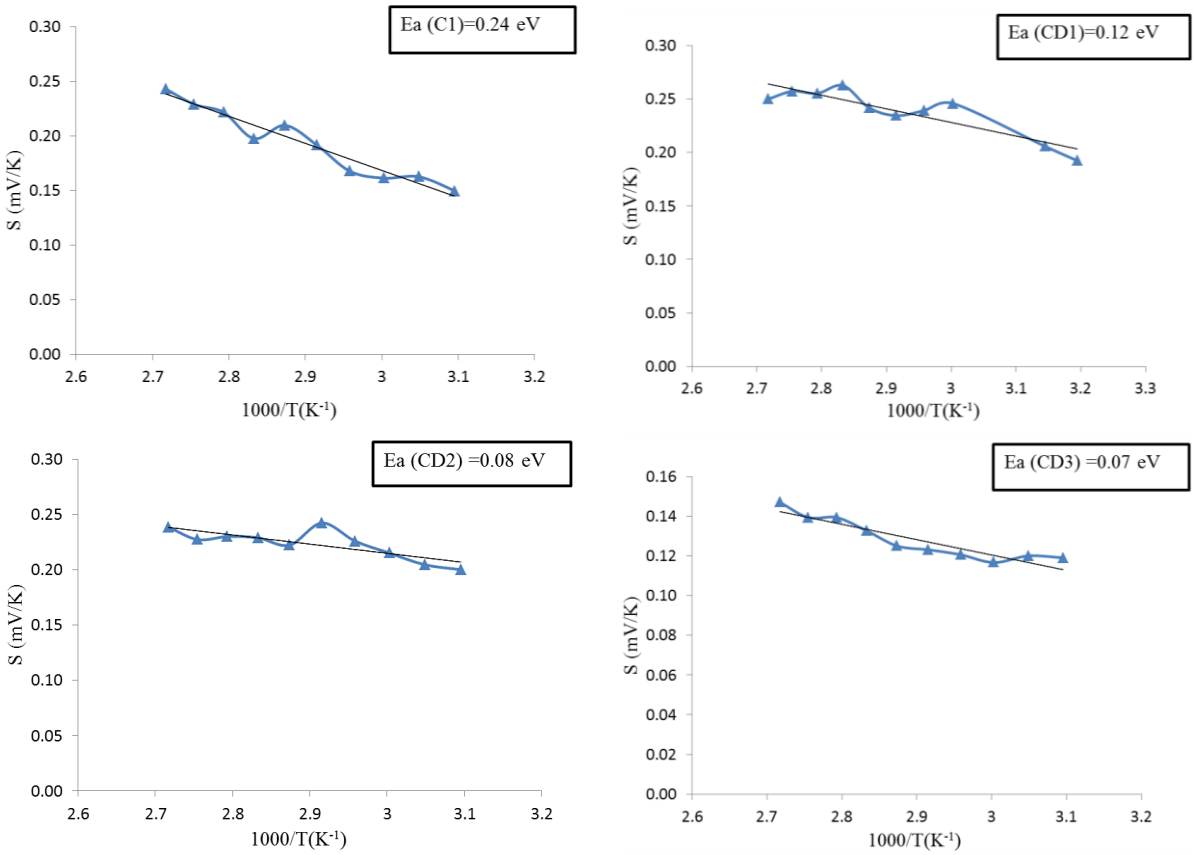

Figure 5. Activation energy for CuO pure(C1) and doping with 3%(CD1), 6%(CD2), and 9%(CD3) Co.

Hall effect measurements is used to calculate carrier density, mobility and conductivity which are listed in Table 3. Increasing of CuO conductivity at 9% doping of Co, due to degradation of CuO Structure.

Table 3. The results of Hall Effect for un-doped and Co- doped COTF.

Sample	Carrier concentration cm^{-3}	Mobility ($cm^2 V^{-1} s^{-1}$)	Condactivty $(\Omega\ cm)^{-1}$	Type of Cuo
CuO-pure	7.4×10^{17}	1.005	0.119	p-type
CuO doping 3% Co	6.3×10^{17}	1.002	0.101	p-type
CuO doping 6% Co	1.1×10^{18}	1.072	0.189	p-type
CuO doping 9% Co	2.2×10^{18}	1.052	0.370	p-type

4. Conclusions

In summary, Co-doped and un-doped COTF were successfully prepared by using spray pyrolysis method. XRD showed monoclinic polycrystalline. However, Co-doped samples showed larger grain size with distortion in the structure. With increasing of doping concentration the structure changes to amorphous. The grain size increases for doping concentration larger than 3%. Bandgab energy of the samples decreases with doping concentration 6%. Un-doped and Co doped CuO have p-type conductivity. Increasing of conductivity of CuO thin films after Co doped gives importance to the CuO in solar cell applications.

References

[1] Hansen, B. J.; Kouklin, N.; Lu, G.; Lin, I. K.; Chen, J.; Zhang, X. "Transport, analyte detection, and opto-electronic response of p-type CuO nanowires"; The Journal of Physical Chemistry C, 114(6), 2440-2447, 2010.

[2] Kumar, D. A.; Xavier, F. P.; Shyla, J. M. "Investigation on the variation of conductivity and photoconductivity of CuO thin films as a function of layers of coating"; Archives of Applied Science Research, 4(5), 2174-2183, 2012.

[3] Li, P.; Xu, J.; Jing, H.; Wu, C.; Peng, H.; Lu, J.; Yin, H. "Wedged N-doped CuO with more negative conductive band and lower overpotential for high efficiency

photoelectric converting CO_2 to methanol"; Applied Catalysis B: Environmental, 156, 134-140, 2014.
[4] Nesa, M. "Characterization of zinc doped copper oxide thin films synthesized by spray pyrolysis technique"; 2016.
[5] Baturay, Ş.; Tombak, A.; Batibay, D.; Ocak, Y. S. "n-Type conductivity of CuO thin films by metal doping"; Applied Surface Science, 477, 91-95, 2019.
[6] Chtouki, T.; Taboukhat, S.; Kavak, H.; Zawadzka, A.; Erguig, H.; Elidrissi, B.; Sahraoui, B. "Characterization and third harmonic generation calculations of undoped and doped spin-coated multilayered CuO thin films"; Journal of Physics and Chemistry of Solids, 124, 60-66, 2019.
[7] Oh, J.; Ryu, H.; Lee, W. J. "Effects of Fe doping on the photoelectrochemical properties of CuO photoelectrodes"; Composites Part B: Engineering, 163, 59-66, 2019.
[8] Zare Asl, H.; Mohammad Rozati, S. "Spray deposited nanostructured CuO thin films: influence of substrate temperature and annealing process"; Materials Research, 21(2), 2018.
[9] Koffyberg, F. P.; Benko, F. A. "A photoelectrochemical determination of the position of the conduction and valence band edges of p-type CuO"; Journal of Applied Physics, 53(2), 1173-1177, 1982.
[10] Kadhim, R. G.; Kzar, K. "Structural and Optical Properties of CuO Doped (Li) Thin Films Prepared by Sol-Gel Technique"; World Scientific News, 56, 56-66, 2016.
[11] Wang, R. C.; Lin, S. N.; Liu, J. Y. "Li/Na-doped CuO nanowires and nanobelts: Enhanced electrical properties and gas detection at room temperature"; Journal of Alloys and Compounds, 696, 79-85, 2017.
[12] Mariammal, R. N.; Ramachandran, K.; Kalaiselvan, G.; Arumugam, S.; Renganathan, B.; Sastikumar, D. "Effect of magnetism on the ethanol sensitivity of undoped and Mn-doped CuO nanoflakes"; Applied surface science, 270, 545-552, 2013.
[13] Chandramohan, R.; Valanarasu, S.; Ganesh, V.; Shkir, M., Kathalingam, A.; AlFaify, S. "Facile synthesis and characterization of undoped, Mn doped and Nd co-doped CuO nanoparticles for optoelectronic and magnetic applications"; Journal of Molecular Structure, 1171, 388-395, 2018.
[14] Mersian, H.; Alizadeh, M.; Hadi, N. "Synthesis of zirconium doped copper oxide (CuO) nanoparticles by the Pechini route and investigation of their structural and antibacterial properties"; Ceramics International, 44(16), 20399-20408, 2018.
[15] Sharma, A.; Dutta, R. K.; Roychowdhury, A.; Das, D.; Goyal, A.; Kapoor, A. "Cobalt doped CuO nanoparticles as a highly efficient heterogeneous catalyst for reduction of 4-nitrophenol to 4-aminophenol"; Applied Catalysis A: General, 543, 257-265, 2017.
[16] Tawfik, W. Z.; Khalifa, Z. S.; Abdel-wahab, M. S.; Hammad, A. H. "Sputtered cobalt doped CuO nano-structured thin films for photoconductive sensors"; Journal of Materials Science: Materials in Electronics, 30(2), 1275-1281, 2019.
[17] Kamble, S. P.; Mote, V. D. "Structural, optical and magnetic properties of Co doped CuO nano-particles by sol-gel auto combustion technique"; Solid State Sciences, 95, 105936, 2019.
[18] Shackelford, J. F.; Han, Y. H.; Kim, S.; Kwon, S. H. "CRC materials science and engineering handbook"; CRC press, pp15, 2016.
[19] Chiang, C. Y.; Shin, Y.; Ehrman, S. "Dopant effects on conductivity in copper oxide photoelectrochemical cells"; Applied Energy, 164, 1039-1042, 2016.
[20] Chaudhary, N. V. P.; Murthy, J. K.; Venimadhav, A. "Absence of dipolar ordering in Co doped CuO"; Solid State Communications, 247, 36-39, 2016.
[21] Bayansal, F.; Taşköprü, T.; Şahin, B.; Çetinkara, H. A. "Effect of cobalt doping on nanostructured CuO thin films"; Metallurgical and Materials Transactions A, 45(8), 3670-3674, 2014.
[22] Bowen, D. K.; Tanner, B. K. "X-ray metrology in semiconductor manufacturing"CRC Press, 2006.
[23] Szekely, F.; Groma, I.; Lendvai, J. "Characterization of self-similar dislocation structures by X-ray diffraction"; Materials Science and Engineering: A, 324(1-2), 179-182, 2002.